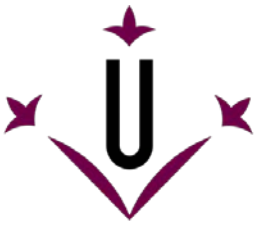

Plant Science 239 (2015) 15–25
doi:10.1016/j.plantsci.2015.07.011

Photosynthesis-dependent/independent control of stomatal responses to CO_2 in mutant barley with surplus electron transport capacity and reduced SLAH3 anion channel transcript

Javier Córdoba[a,b], José-Luis Molina-Cano[b,1], Pilar Pérez[a], Rosa Morcuende[a], Marian Moralejo[c], Robert Savé[d], Rafael Martínez-Carrasco[a*]

[a]Institute of Natural Resources and Agrobiology of Salamanca, IRNASA-CSIC, Cordel de Merinas 40, E-37008 Salamanca, Spain
[b]IRTA (Institute for Food and Agricultural Research and Technology), Field Crops, Av. Alcalde Rovira i Roure, 191, E-25198 Lérida, Spain
[c]Universidad de Lleida, Av. Alcalde Rovira i Roure, 191, E-25198, Lérida, Spain
[d]IRTA, Environmental Horticulture, Torre Marimon, E-08140 Caldes de Montbui, Barcelona, Spain
[1]Retired

[*]Corresponding author:

Rafael Martínez-Carrasco

Phone: +34 923 219606

E-mail address: rafael.mc@csic.es

Abstract

The mechanisms of stomatal sensitivity to CO_2 are yet to be fully understood. The role of photosynthetic and non-photosynthetic factors in stomatal responses to CO_2 was investigated in wild-type barley (*Hordeum vulgare* var. Graphic) and in a mutant (G132) with decreased photochemical and Rubisco capacities. The CO_2 and DCMU responses of stomatal conductance (g_s), gas exchange, chlorophyll fluorescence and levels of ATP, with a putative transcript for stomatal opening were analysed. G132 had greater g_s than the wild-type, despite lower photosynthesis rates and higher intercellular CO_2 concentrations (C_i). The mutant had Rubisco-limited photosynthesis at very high CO_2 levels, and higher ATP contents than the wild-type. Stomatal sensitivity to CO_2 under red light was lower in G132 than in the wild-type, both in photosynthesizing and DCMU-inhibited leaves. Under constant C_i and red light, stomatal sensitivity to DCMU inhibition was higher in G132. The levels of a SLAH3-like slow anion channel transcript, involved in stomatal closure, decreased sharply in G132. The results suggest that stomatal responses to CO_2 depend partly on the balance of photosynthetic electron transport to carbon assimilation capacities, but are partially regulated by the CO_2 signalling network. High g_s can improve the adaptation to climate change in well-watered conditions.

Key words: CO_2, *Hordeum vulgare*, photosynthetic electron transport, signalling, SLAH3, stomatal conductance

Abbreviations: A, rate of CO_2 assimilation; A_c, rate of CO_2 assimilation limited by Rubisco; A_j, rate of CO_2 assimilation limited by RuBP regeneration; C_a ambient CO_2 concentration; C_i, intercellular CO_2 concentration in leaves; DCMU, 3-(3,4-dichlorophenyl)-1,1-dimethylurea; Fv/Fm, maximum quantum efficiency of PSII photochemistry; Fq'/Fm', PSII operating efficiency; Φ_{NPQ}, quantum yield of non-photochemical quenching; g_s, stomatal conductance; J, potential rate of photosynthetic electron transport; PSII, photosystem II; qL, fraction of PSII centres which are in the open state; qRT-PCR, quantitative real-time polymerase chain reaction; RuBP, Ribulose-1, 5-bisphosphate; Rubisco, Ribulose-1, 5-bisphosphate carboxylase/oxygenase; SBPase, sedoheptulose-1, 7-bisphosphatase; V_{cmax}, maximum rate of Rubisco-catalyzed carboxylation; WT, wild-type.

1. Introduction

Stomata provide plants with a key mechanism for regulating water loss and CO_2 uptake, and constantly adapt to a changing environment. Diverse factors control stomatal opening and closure ([1-5] and earlier references therein [6, 7]). Stomatal conductance and the CO_2 assimilation rate are often correlated in such a way that the ratio of intercellular (C_i) to ambient (C_a) CO_2 concentrations is almost constant [8, 9], although it may be modified by certain environmental factors [8]. By altering C_i while C_a was held constant, and by altering C_a while C_i was held constant, the stomata were shown to respond to C_i and to be insensitive to C_a [10]. C_i alone is unable to regulate the correlation between CO_2 assimilation and g_s [11], and the underlying mechanism is still unclear. It has been hypothesized that the C_i response of g_s is controlled by the balance between electron transport capacity and Ribulose-1, 5-bisphosphate carboxylase oxygenase (Rubisco) carboxylation [8], either in the guard cells or in the mesophyll. Alternatively, the redox state of the photosynthetic electron transport components [12] may regulate this response. An increase in electron transport capacity and associated products, such as ATP, NADPH or Ribulose-1, 5-bisphosphate relative to Rubisco capacity [13, 14], or the greater reduction in plastoquinone and upstream electron transport components [12], would increase g_s. Photosynthetic electron transport could provide the ATP required for H^+ pumping and cation uptake at the guard-cell plasma membrane [15]. Alternatively, a yet unknown signalling pathway could link the redox state of the electron transport chain to stomatal movements [12]. In contrast with this hypothesis, transgenic plants with low aldolase [16], fructose-1,6-bisphosphatase [17], glyceraldehyde-3-phosphate dehydrogenase [18], Rubisco or cytochrome b_6f content [19-22], in which CO_2 assimilation is inhibited but g_s is similar to the wild-type (WT), suggest that stomatal conductance is not directly determined by the photosynthetic process [19, 22]. Nevertheless, in sedoheptulose-1, 7-bisphosphatase (SBPase) antisense mutant plants, in which the regenerative capacity of the Calvin-Benson cycle decreased with no effects on carboxylation efficiency, the closing response of the stomata to increasing C_i was decreased relative to the WT [23]. This mutation could result in increased levels of chloroplastic ATP. Prior work with transgenic plants with strong reductions in Rubisco activity and photosynthetic capacity [19, 22] was performed in growth chambers at elevated CO_2 concentrations (800 or 953 μmol mol^{-1}), which can

affect stomatal sensitivity to CO_2 [24-26]. Similarly, studies on the contribution of photosynthesis to the red light response of stomatal conductance involved plants with antisense reductions in the cytochrome b_6f complex [19] grown under very low light intensity (25 μmol m^{-2} s^{-1}), which alters the relative stoichiometries of the thylakoid protein complexes [27]. In turn, antisense SBPase plants grown in normal air under glasshouse conditions had only a small difference with the WT in conductance response to increasing C_i [23]. These earlier results prompted us to study the effects of photosynthesis on stomatal CO_2 responses in an ambient CO_2 concentration, under both growth chamber and glasshouse lighting. We compared the WT with a barley mutant with lower photosynthesis, but distinctly higher stomatal conductance. Stomatal movements were measured under red light, which shares characteristics of photosynthesis in its action spectrum in the red region, while blue light is perceived by phototropins and induces stomatal opening by a different mechanism [19].

The Photosystem II electron transport inhibitors 3-(3,4-dichlorophenyl)-1,1-dimethylurea (DCMU) [9, 14, 15] and cyanazine (2-chloro-[l-cyano-l-methylethylamino]-6- ethylamino-S-triazine) [9] and the carotenoid synthesis inhibitor norflurazon [28, 29] have been used to examine the dependence of stomatal conductance on photosynthesis. These compounds decreased g_s and enhanced its response to rising CO_2 in *Gossypium hirsutum* [9], and brought g_s down to nearly zero in *Xanthium strumarium* when photosynthetic electron transport was completely blocked all over the leaf [14]. These results suggest that stomata respond to changing CO_2 concentrations through a mechanism that depends on photosynthetic electron transport. However, in the absence of electron transport the stomata retain a response to C_i [14, 28, 29], pointing to a second mechanism that does not depend on photochemical reactions. Indeed, stomatal guard cells can directly sense C_i [10, 29]. The existence of an additional photosynthesis-unrelated pathway contributing to CO_2-induced stomatal movements is evidenced by work with mutants lacking components of the CO_2 signalling network in guard cells: carbonic anhydrases such as βCA1 and βCA4 in Arabidopsis [28], the HT1 (HIGH LEAF TEMPERATURE 1) protein kinase [30, 31], the S-type anion channels SLAC1 [5, 31, 32] and SLAH3 [33], the OST1 and CPK family protein kinases [33, 34] involved in activating these anion channels, GCA2 (growth controlled by abscisic acid 2) and the ABCB14 malate transporter [35]. Altered stomatal sensitivity to CO_2 in mutants with reduced photosynthetic capacity, but normal

or high conductance, could be due to changes in the components of the CO_2 signal transduction pathway in guard cells.

The first aim of this work was to further investigate whether the CO_2 response of g_s is controlled by the balance between electron transport capacity and carboxylation by Rubisco. Our approach was to compare with the barley WT a sodium azide mutant (G132) with low photosynthesis rates, but high stomatal conductance. The experiments were carried out both in growth chamber and glasshouse to identify environment-independent responses. The photosynthetic and non-photosynthetic controls of gs were distinguished by inhibiting electron transport with DCMU, and by assessing the CO_2 response of gs in photosynthesizing and DCMU-poisoned leaves of the mutant and the WT. The second aim of our research was to appraise the role of the guard cell CO_2 signalling network on the altered gs responses to CO_2 in G132. With this purpose, we screened a differential expression of genes for components of that network.

2. Material and Methods

2.1. Plant material and growing conditions

Barley (*Hordeum vulgare* L.) pure pedigree seed of the Graphic variety (WT) and homozygous, sodium azide mutagenized seeds of the line G132 were obtained from Dr J. L. Molina-Cano's mutant collection at IRTA. An initial characterization of the mutant has been reported [36] and the study of the exome capture of the mutant compared with the WT is currently in progress. Preliminary gas exchange measurements revealed that G132 had lower photosynthesis and higher g_s than the WT. Seeds of G132 and WT were surface sterilized with hypochlorite and sown in 5 L pots with 1.2 kg of peat: perlite (4:1) substrate, with a density of four plants per pot after emergence. Four g of KNO_3 and 4 g of KH_2PO_4 were added to each pot. The peat provided a sufficient supply of other nutrients. Water was supplied during growth to maintain pot field capacity. The plants were grown in a controlled environment chamber or a glasshouse. Chamber conditions were as follows: ambient CO_2, 450 μmol m^{-2} s^{-1} irradiance at the top of the canopy, 16:8 h light:dark photoperiod, 20:15 ºC light:dark temperatures, and 60±5 % relative humidity. The glasshouse had partial temperature control to achieve *c*. 20:15 ºC day:night temperatures, supplementary illumination to extend the photoperiod to 16 h with a minimum of 400 μmol m^{-2} s^{-1} irradiance, and 60±10 % relative humidity. All measurements were performed on the youngest fully expanded leaf, at the developmental stages of 3-4 leaves or 5-7 leaves (13-14 or 15-17 stages of the Zadoks scale [37]), with WT being more developed than G132.

2.2. *Chlorophyll fluorescence and gas exchange*

The chlorophyll fluorescence quenching analysis followed the procedure described by Pérez et al. [38]. Leaf sections were kept in the dark for 20 min with leaf clips, after which dark-adapted state fluorescence parameters were measured. Fo was recorded and a saturating flash of light (~8000 μmol m^{-2} s^{-1}) was applied for 0.8 s to determine Fm. Fo and Fm, respectively, represent the minimal and maximal fluorescence in the dark-adapted state, and Fv/Fm [(Fm–Fo)/Fm] represents the maximum quantum efficiency. Light-adapted leaves were illuminated with the red actinic light source of the fluorometer to obtain an irradiance of 1000 μmol m^{-2} s^{-1}. Saturating light pulses were

given every 20 s until steady-state chlorophyll fluorescence parameter values were obtained, the fluorescence values being recorded immediately before (F', steady-state fluorescence) and after (Fm', maximal fluorescence in the light) each pulse. Then, the leaf was covered with a black cloth, the actinic light was switched off, and an infrared light was switched on for 3 s to quickly reoxidize the Photosystem II (PSII) centres and measure Fo', the minimal fluorescence with a non-photochemical quenching (NPQ) similar to that found in the steady-state under light. The equipment determines Fq'/Fm' [(Fm'–F')/Fm'], which is the PSII operating efficiency (also termed Φ_{PSII}). The fraction of PSII centres in the open state, qL, equates to (Fq'/Fv')(Fo'/F'). The quantum yield of non-photochemcial quenching, Φ_{NPQ}, is 1–(Fq'/Fm')–Φ_{NO}, where Φ_{NO}, the quantum yield of basal, non-radiative decays is 1/[NPQ+1+qL(Fm/Fo–1)] and NPQ is (Fm/Fm')–1. Chlorophyll fluorescence was measured in five replicate leaves (from different plants) of each genotype at the stage of 3 (G132)-4 (WT) leaves from glasshouse-grown plants.

Gas exchange was measured in the central segment of leaves using a 1.7 cm^2-window leaf chamber connected to an infrared gas analyser (PLC6 [rice] and CIRAS-2, respectively, PP Systems, Amesbury, MA, USA). The air flow rate was 300 ml min^{-1}, leaf temperature was kept at 20 ºC using the Peltier system in the leaf chamber, irradiance was set at 1000 µmol m^{-2} s^{-1} provided by red supplemented with white LEDs, with a 0.95±0.12 kPa vapour pressure deficit. The gas exchange-CO_2 response curves were recorded by decreasing CO_2 concentration in five steps from 390 to 60 µmol mol^{-1} (*c*. 10 min), followed by an increase from 390 to 1800 µmol mol^{-1} (*c*. 15 min) in six steps. At each step, as soon as the chamber's CO_2 concentration was stable, but not necessarily steady-state (*c*. 2 min), the gas exchange parameters were recorded [39]). The photosynthesis-C_i responses were used to determine the maximum rate of Rubisco-catalyzed carboxylation (V_{cmax}), the potential rate of photosynthetic electron transport (J) and the limitations of photosynthesis by Rubisco, Ribulose-1, 5-bisphosphate (RuBP) regeneration or Triose-phosphate utilization, according to Farquhar et al. [40]. This model was fitted with the LeafWeb utility [41]. These short-term CO_2 responses were measured in five youngest fully expanded replicate leaves of each genotype at the stages of 3 (G132)-4 (WT) leaves from both a growth chamber and a glasshouse, and of 5 (G132)-7 (WT) leaves from a glasshouse. Measurements are presented for glasshouse plants at the earlier stage of development; similar results were obtained in other recordings.

The long-term responses of g_s and other gas exchange parameters to CO_2 concentration were recorded for 40-50 min by first equilibrating the leaves in 1000 μmol m^{-2} s^{-1} irradiance and 390 μmol mol^{-1} CO_2 for 20 min, and then increasing or decreasing CO_2, respectively, to 1800 or 40 μmol mol^{-1} in a single step. For the quantitative comparisons of the genotypes, we calculated the stomatal responses as ratios of final to initial g_s for the recording time, and determined the response kinetics with functions of best fit and derivatives with respect to time, as detailed in section 2.7. To distinguish the stomatal responses to CO_2 from those induced by blue light [42], these long-term measurements were carried out under red light illumination, obtained by interposing a long pass optical filter between the lamp and the leaf chamber window. Measurements were replicated in five leaves per genotype from both a growth chamber and a glasshouse experiment, at the same growth stages as for short-term responses to CO_2.

2.3. *Gas exchange of DCMU-treated leaves*

To assess the effects of DCMU on g_s and photosynthesis, the youngest fully expanded leaves (six replicate leaves per genotype) from glasshouse-grown plants at the 5-leaf stage (Zadoks scale 15) for both genotypes were detached and cut under water with a sharp scalpel, and then the cut base was placed in water containing 1.5 % ethanol (for adequate comparison with the subsequent DCMU treatment; see below). The central section of the leaf was inserted into the gas exchange leaf chamber (1.7 cm^2) for equilibration for 30 min at 400 μmol mol^{-1} CO_2 and 1000 μmol m^{-2} s^{-1} red irradiance. The leaf base was then rapidly transferred into 100 μM DCMU in ethanol [15] (or into 1.5 % ethanol for the controls); we found that 1.5 % was the minimum ethanol concentration required to dissolve DCMU. Preliminary measurements indicated that photosynthesis reached the CO_2 compensation point in less than 90 min; thus, gas exchange data were recorded for *c*. 2 h. Although previous experiments indicated that the response to DCMU was similar when C_i was allowed to vary during leaf incubations, the initial C_i value was kept approximately constant by decreasing C_a to ensure that DCMU responses were not the result of increases in C_i. Subsequently, CO_2 concentration was lowered to 50 μmol mol^{-1} and recordings continued for 90 min, following which CO_2 was increased to 800 μmol mol^{-1} and measurements continued for

100 min. The magnitudes and rates of stomatal responses were determined as described in section 2.2.

2.4. *Stomatal density and index of leaves*

Preliminary recordings indicated that stomatal density was 21 % higher on the adaxial than on the abaxial side of the leaves. The stomatal and epidermal cell numbers on the adaxial side of similar leaves to those used for gas exchange measurements were determined from impressions with nail polish. The stomata were counted in 1.8 mm^2 fields of view with a compound microscope using a magnification of 112.5. Ten fields of view regularly spaced along leaves in a glasshouse crop and five fields of view from the central segment of leaves in a growth chamber crop were counted in five replicate leaves per genotype at the growth stages indicated above. The stomatal index was the ratio of stoma to pavement cell numbers. Conductance was normalized to the stomatal density of the leaves by dividing the steady state g_s by the number of stomata per unit area; the steady state g_s was that attained after 20 min equilibration period at 390 µmol mol^{-1} CO_2 and 1000 µmol m^{-2} s^{-1} red light irradiance (see section 2.2). This approximation was taken as valid for comparative purposes, even though the conductance of the whole leaf would overestimate g_s for stomata on the adaxial surface.

2.5. *ATP contents*

At mid-morning in the growth stage of 3-4 leaves of plants grown in a controlled environment chamber, five replicate samples of the youngest fully expanded leaves per genotype, each consisting of five leaves, were harvested; each leaf was cut, immediately plunged into liquid nitrogen under illumination and then stored at -80 ºC until analysed. Subsamples of 150 mg were ground in a chilled mortar and extracted with 1 M $HClO_4$ with 5 mM EGTA for 30 min on ice, with frequent shaking. After centrifugation at 13000 g at 4 ºC for 5 min, the supernatant was collected and the precipitate was washed with water, centrifuged, and the supernatant was added to the perchloric acid extract. The combined extract was then neutralized with 5 M KOH- 1 M triethanolamine pH 7.0, centrifuged at 13000 g at 4 ºC for 5 min, the supernatant was collected, and the precipitate washed with water, centrifuged, and the supernatants were pooled. Extracts were not clarified with charcoal, which would remove the adenylates. ATP was analysed by the Lowry and Passonneau method [43], with glucose, hexokinase, glucose-

6-P isomerase, NADP and glucose-6-P dehydrogenase, and measuring NADPH formation by the change in absorbance at 340 nm minus 400 nm. ATP recovery was determined by comparing the analyses of extracts with and without the addition of representative amounts of ATP standard.

2.6. *Transcript profiling*

Microarray processing was performed on the primary leaf RNA extracts from six replicates per genotype, using Agilent 56k barley microarray. Each replicate consisted of three-five primary leaves from plants grown in a controlled environment chamber harvested at the 2-leaf stage (Zadoks scale 12). Probe design, labelling and hybridization were performed at the Leibniz Institute of Plant Genetics and Crop Plant Research (IPK, Gatersleben, Germany). The arrays were scanned at a 2-micron high resolution using the DNA Microarray Scanner G2565CA (Agilent), and statistically analysed with GeneSpring (v 12) software (Agilent). The results from the analysis of these microarrays will be reported in full elsewhere. The sequence of a transcript potentially involved in stomatal aperture, which was differentially expressed (see below) in G132 relative to WT, was compared and annotated using the HarvEST, GenBank and Mercator tools [44-46]. The results were validated by quantitative real-time polymerase chain reaction (qRT-PCR).

Based on the results of the microarrays, the levels of transcript for a protein (SLAH3-like) putatively involved in the regulation of stomatal aperture were determined by qRT-PCR in five replicates, each consisting of five youngest fully expanded leaves of each genotype, at the stages of 3 (G132)-4 (WT) leaves from controlled environment-growth plants and of 5 (G132)-7 (WT) leaves from glasshouse-grown plants. Analyses were performed in duplicate. RNA extraction and purification followed the procedure described by Morcuende et al. [47]. Primers were designed for a barley SLAH3 slow anion channel (GenBank: AK368060, forward CCAACACAAGCAGCAAGACC, reverse GAAGCCGTCGAGATGGGAAA). Total RNA was treated with TURBO DNase (Ambion) before proceeding with the cDNA synthesis using the SuperScript III Reverse Transcriptase (Invitrogen) according to the manufacturer's instructions. The qRT-PCR assays were performed in 384-well plates with a sequence detector system (ABI PRISM 7900 HT, Applied Biosystems), using Power SYBR Green PCR Master Mix (Applied Biosystems), cDNA and gene-specific primers in a total volume of 10 µl.

The thermal profile was as follows: 50 ºC for 2 min and 95 ºC for 10 min, followed by 40 cycles of 95 ºC for 15 s, then 60 ºC for 1 min, and a final temperature increase from 60 ºC to 95 ºC at 1.9 ºC min^{-1}. For normalization, the genes were used of ubiquitin (GenBank: M60175, forward CACCCTCGCCGACTACAA and reverse CTTGGGCTTGGTGTACGTCT primers) and actin (GenBank: AY145451, forward GGCACACTGGTGTCATGG and reverse CTCCATGTCATCCCAGTT primers). The formation with each primer pair of a single PCR product of the expected size was assessed by agarose electrophoresis and PCR melting curve data. Relative quantification used the comparative C_t (threshold cycle) method ($2^{-\Delta\Delta Ct}$, Schmittgen and Livak, [48]).

2.7. Statistical analyses

The data were subjected to analyses of variance with no blocking (GenStat 6.2). The rates of stomatal closure or opening in response to long-term changes in CO_2 concentration and to DCMU feeding were compared by fitting the empirical functions of best fit among a series of standard curves to the g_s kinetics over time. Regressions with groups (analysis of parallelism, GenStat 6.2) were analysed to determine whether a common regression should be fitted for the two genotypes (implying that there was no difference between them), or whether regressions with some or all their parameters separated should be selected (indicating that the kinetics differed in elevation or slope). To fit the functions, all five or six replicate leaves from each genotype were included separately. Stomatal opening and closing rates were estimated as first derivatives of the selected functions with respect to time. The microarray data were processed using GeneSpring (v.12) software (Agilent). A statistical filter was applied to the data, which were subjected to an analysis of variance (P value<0.01) with Benjamini and Hochberg correction [49] for false positives (FDR).

3. Results

3.1. Functional features of the G132 mutant

The G132 mutant had a lower PSII maximum (Fv/Fm) and operating (Fq'/Fm') quantum efficiencies than WT (Table 1). Since qL did not significantly vary between genotypes, the mutant's decreased Fq'/Fm' was due to the lower quantum efficiency of open PSII centres. Indeed, the quantum yield of non-photochemical quenching (Φ_{NPQ}) increased in G132 relative to WT. ATP is a major product of electron transport in chloroplasts and mitochondria; its concentration in whole extracts of young fully expanded leaves was significantly higher in the mutant than in WT (Table 1). In addition, G132 had low chlorophyll and Rubisco protein contents (data not shown). Remarkably, V_{cmax} limited G132 photosynthesis up to 1800 μmol mol^{-1} air CO_2 concentration, in contrast with the expected J limitation of photosynthesis at high CO_2 observed in WT (Fig. 1). Thus, G132 had a surplus electron transport capacity. In the youngest fully expanded leaves, at different plant development stages (both growth chamber (Fig. 2a) and glasshouse environments (Fig. 2b, c)), photosynthesis rates measured in ambient CO_2 and high light intensity were lower in G132 than in WT. In spite of its inferior photosynthetic performance, G132 had a higher stomatal conductance than WT (Fig. 2).

3.2. Stomatal density and index of leaves

In plants grown in a controlled environment chamber, the stomatal density on the adaxial central segment of the leaves was found to be higher in G132 than in WT (Fig. 3a). In glasshouse-grown plants, stomatal density increased from leaf base to apex in both genotypes, and was higher in G132 than in WT (Fig. 3b), thus confirming the result of the prior experiment. There was no genotypic difference in stomatal index in the younger, controlled environment-grown plants (Fig. 3a), but there was a small (13.5 %) yet significant increase in the stomatal index in G132 compared to WT glasshouse-grown plants (Fig. 3b). Greater numbers of stomata per unit leaf area, and a similar or marginally higher stomatal index in the mutant, imply that stomatal size was smaller in G132 than in WT. To verify whether the greater g_s of G132 was due solely to the higher density of stomata, steady state (after about 20 min) g_s with ambient CO_2 concentration and high irradiance was normalized to stomatal density on the central segment of the leaves (see section 2.4). The normalized conductance was similar in both genotypes in

plants from the growth chamber (Fig. 3c), but greater in G132 than in WT in plants grown in the glasshouse (Fig. 3d) and measured at a later developmental stage. Thus, depending on plant age or the growth environment (not obvious from the data), the higher g_s of G132 is attributable to greater stomatal aperture or even to greater stomatal density.

3.3. Stomatal responses to CO_2

Stomatal conductance responds in general more slowly to changes in conditions than photosynthesis [50]. Therefore, the gas exchange parameters were determined for 40-50 min following a step increase in the ambient CO_2 concentration up to 1800 μmol mol^{-1} under high intensity red light. Photosynthesis initially increased in WT, mostly in plants grown in a controlled environment chamber, and then remained stable (Fig. 4a, b). No increase in photosynthesis was observed in G132 during measurements. Whilst there were large genotypic differences in the photosynthesis of the 3^{rd}-4^{th} leaf in growth chamber plants, WT had only marginally higher photosynthesis than G132 in the 5^{th} (G132)-7^{th} (WT) leaves on glasshouse plants. This difference in the magnitude of the change between genotypes was also observed in short-term measurements of photosynthesis, and is attributable to plant age, rather than to the growth environment (compare Figs. 2a and 2b with Fig. 2c). This result shows a gradual recovery of photosynthetic capacity in the mutant. Intercellular CO_2 concentration decreased further to a steady state in WT than in G132 (Fig. 4c, d), which had higher C_i. In both growth conditions, the fractional decrease in g_s after 40-50 min in the elevated CO_2 concentration was lower in G132 than in WT (Fig. 5a, b). The kinetics of stomatal response was also slower in the mutant (Fig. 5c, d). Indeed, the regressions of g_s over time ($g_s=A+B\cdot\exp^{(k\cdot time)}+C\cdot time$) were significantly different for both genotypes (Table 2), with lower rates of stomatal closure for the mutant (Fig. 5e, f). Therefore, g_s sensitivity to an increase in CO_2 was lower in G132 than in WT. When decreasing the CO_2 concentration from 390 to 50 μmol mol^{-1}, the stomatal conductance of the youngest fully expanded leaves changed little in both genotypes during the following 40-50 min (data not shown).

3.4. Stomatal and photosynthetic responses to DCMU and CO_2

The role of photosynthesis on stomatal aperture was also investigated by feeding detached leaves with the PSII inhibitor DCMU. The initial C_i was kept constant (278±6 and 223±8 μmol mol^{-1} for G132 and WT, respectively) under bright red light. Photosynthesis gradually declined after about 10 min of 100 μM DCMU treatment, reaching the CO_2 compensation point about 90 min later (Fig. 6a). Stomatal conductance increased for 20-30 min – for longer in WT than in G132 – after transfer to DCMU, and then decreased gradually. The ratio of final to initial g_s was lower in G132 than in WT (Fig. 6c), with the rate of g_s decrease being significantly faster in the former (Table 2; Fig. 6e). Subsequently, once photosynthesis had been fully inhibited, CO_2 concentration was lowered to 50 μmol mol^{-1}. At this point, stomatal conductance (Fig. 6b) increased in both genotypes to the same extent and rate (Fig. 6f; Table 2). About 100 min after the decrease in CO_2, this concentration was raised to 800 μmol mol^{-1}, causing a rapid drop in g_s to very low values in about 90 min (Fig. 6b). The fractional decrease in stomatal conductance was slightly, albeit significantly, greater (Fig. 6d), while the rate of decrease was significantly slower in the mutant than in WT (Table 2; Fig. 6f).

3.5. Correlation of transcripts with the regulation and movements of stomata

The analysis of the 56k barley microarrays for primary leaves of plants grown in a controlled environment chamber showed in G132, relative to WT, a strong decrease in the transcript abundance of unigene 38703 (HarvEST: Barley v.1.83, Assembly 35). This gene has a high identity (NCBI) with the *Hordeum vulgare* accession AK368060. The transcript was annotated (Mercator) and manually curated (UniProtKB/Swiss Prot) as a SLAC1-like (SLAH3) slow anion channel (Table 3), a component of the guard cells signalling network for stomatal closure in response to CO_2 [32, 34]. Quantitative RT-PCR for leaves similar to those used for the gas exchange measurements of controlled environment and glasshouse plants confirmed the lower SLAH3 transcript level in G132 than in WT (Table 3); this genotypic difference was smaller for the older, glasshouse-grown plants than for leaves at an earlier growth stage growing in a controlled environment chamber.

4. Discussion

The reduced photosynthesis of G132 compared to WT (Figs. 2, 4a) was associated with increased intercellular CO_2 concentration (Fig. 4c, d), which together would be expected to decrease stomatal conductance [10]. The higher g_s of the mutant (Figs. 2a-c and 5c, d) contradicts this expectation. The similar or greater conductance normalized to stomatal density in G132 than in WT (Fig. 3c, d) dismisses the possibility of the mutant's higher g_s being due to a greater number of stomata (Fig. 3a, b) with a smaller aperture. With ambient, rather than elevated, growth CO_2 [22], and both glasshouse and controlled environment light intensities rather than dim light [19], leaves of G132 at different plant developmental stages also had lower extent (Fig. 5a, b) and rate (Fig. 5e, f) of stomatal closure than WT in response to rising atmospheric CO_2. From these results it may be firmly concluded that the low-photosynthesis mutant G132 has reduced sensitivity to high CO_2. The speed of stomatal responses to environmental signals is important for identifying regulating mechanisms [33] and maximizing CO_2 uptake [51].We have assessed the response time of g_s to CO_2 through the selection and statistical comparison of curves of best fit, and have derived rates for each genotype from the start of CO_2 change to the final steady state. This may be preferable to determining only maximum rates [33] or linear response rates after a first phase [22].

Previous studies suggest that smaller stomata may respond to environmental changes more quickly than larger ones [51, 52]. The opposite result with G132, which had smaller stomata compared to WT, shows that functional factors may have a greater influence on guard-cell movements than anatomical characteristics. Like G132 stomata, those of transgenic plants with impairments in several steps of the photosynthetic process maintain normal, rather than reduced, conductance [19-21, 23]. However, the magnitude and rate of stomatal opening in response to red light – which has an action spectrum similar to that of photosynthesis and the absorption spectrum of chlorophyll [42] – was not affected by antisense reductions in cytochrome b_6f complex and Rubisco [19]. These results have led to the conclusion that g_s is not directly determined by photosynthetic capacity or chloroplastic electron transport in guard cells or the mesophyll. On the other hand, the reduced stomatal sensitivity to rising CO_2 observed in G132 has also been found, albeit to a small extent, in SBPase antisense tobacco mutants, which could have increased levels of chloroplastic electron transport products such as ATP [23]. The high yield of non-photochemical quenching in the G132 mutant

(Table 1) could be due to an increase in the proton gradient across the thylakoids, caused by the low consumption of electron transport products due to the slow rate of carbon assimilation. This would lead to ATP and NADPH build-up. Our experimental results indicate that ATP concentration in all the illuminated leaves, and very likely in chloroplasts [53], was higher in G132 than in WT (Table 1). Moreover, the photosynthesis-C_i response of G132 (Fig. 1) was Rubisco-limited up to very high CO_2 concentrations, as found in transgenic tobacco plants with an antisense gene directed against the Rubisco small subunit [20]. This result clearly shows a greater balance between electron transport and carbon fixation capacities. Thus, the G132 barley mutant's responses of g_s to CO_2 are consistent with Farquhar and Wong's stomatal function model [8], relating the higher conductance and reduced CO_2 sensitivity of stomata to the balance of the production and consumption of the products used in carbon assimilation, such as ATP [8, 14, 54, 55]. These responses are also consistent with a positive role in g_s of the reduction in plastoquinone and upstream electron carriers [12]. Higher levels of photosynthetic electron transport products such as ATP could promote stomatal opening [15]. Alternatively, increases in these products, or a reduction in the electron transport chain, could trigger a signalling mechanism, which might modify the levels of a gaseous ion produced in the mesophyll that could reach the guard cells [56]. Although the short-term responses (i.e., standard photosynthesis-CO_2 curves) of g_s to decreases in CO_2 also seemed smaller in G132 than in WT, there was hardly any long-term stomatal opening response to low CO_2 in our experiments (data not shown). The models and experimental data [8, 14, 54] show that when carboxylation is limited by Rubisco and has surplus electron transport capacity, as normally occurs at low CO_2 and high irradiance, g_s is nearly insensitive to CO_2.

Another line of evidence showing that photosynthesis mediates in the stomatal response to CO_2 is the decline in g_s following DCMU feeding (Fig. 6a), which is consistent with prior studies [9, 14, 15, 29]. In our experiments, DCMU was supplied at constant C_i, ruling out the involvement of stomatal closure mechanisms that respond directly to the increase in CO_2 concentration. The gradual decline in CO_2 assimilation with DCMU was probably due to the progressive spread of the inhibitor along the leaf, rather than an even decline of photosynthesis in the whole leaf, in agreement with Messinger et al. [14]. At variance with these authors, however, in our study g_s did not decrease in step with photosynthesis, but had a delayed response to DCMU. Either more time is required for DCMU to reach the stomatal guard cells than other leaf cell types,

or the photosynthesis stimulus over g_s is displaced over a greater distance, whereby the perception of its suppression is delayed. Previous reports support the fact that the stomatal response to CO_2 is caused by a signal generated in the mesophyll [42, 57-59], which could account for the deferred response of g_s to the inhibitor. The earlier and greater (rate and extent) DCMU effect on g_s in G132 than in WT may be due mainly to the disappearance with the inhibitor of the surplus electron transport capacity relative to the carbon assimilation of the mutant. To a lesser extent, it may also be due to the moderately higher (24 %) C_i in G132 than in WT, which could have a photosynthesis-independent effect on stomatal closure.

The stomatal effects of CO_2 on DCMU-treated leaves (Fig. 6b, d) clearly show another mechanism controlling the movements of stomata that is independent of photosynthesis, in agreement with Messinger et al. [14] and Kim et al. [35], and is probably related to CO_2 signalling in guard cells [57]. In contrast with the results reported by Fujita et al., [57], the stomata of DCMU-treated leaves responded to CO_2 under red light, with the reasons for this discrepancy being unclear. In DCMU-poisoned leaves, the extent of stomatal closure in response to an increase in CO_2 concentration was somewhat greater in G132 than in WT (Fig. 6b), although the stomatal response in absolute units was smaller, and the rate of stomatal closure slower in the former (Fig. 6d). Gene expression analysis showed a decrease in G132 compared to WT in transcript abundance for the SLAH3 slow anion channel (Table 3). The efflux of osmoregulatory anions from guard cells via SLAC1 [60] and SLAH3 [34, 60] initiates stomatal closure [61], and affects the sensitivity of K^+ influx channels to cytosolic free Ca^{2+} concentration [60]. The Arabidopsis slac1-7 mutant with a Ser-120 substitution by Phe has a similar stomatal conductance to WT, albeit a slower stomatal closure rate than the latter in response to CO2 [33]. In contrast, the *slac1-3* loss of function mutation in SLAC1 had significantly higher g_s than WT, in addition to reduced sensitivity to elevated CO_2 [33]. As with mutations in the SLAC1 anion channel [62, 63], the decreased abundance of SLAH3 may account for the impaired closure rate of the stomata of G132 in response to increases in the CO_2 concentration in DCMU-treated leaves. The reductions in SLAH3 might be expected to slow stomatal opening in G132 when C_a was decreased to 50 μmol mol^{-1} (Fig. 4b, c), due to the down-regulation of the K^+ influx following the elevation of the cytosolic Ca^{2+} concentration [62, 63]. The Ca^{2+} concentration in G132 may not have increased sufficiently to affect the rise in g_s in

response to low CO_2. Electrophysiological studies are needed to confirm that the levels of SLAH3 protein in G132 decrease in parallel to transcript levels.

The data presented here show that the altered stomatal CO_2 responses of the barley G132 mutant may be due to its surplus electron transport capacity. This suggests that decreased stomatal sensitivity to increases in CO_2 is positively associated to the balance between photosynthetic electron transport and Rubisco-catalysed carboxylation. The operation of a photosynthesis-independent mechanism contributing to CO_2-induced stomatal movements is evidenced by stomatal closure and CO_2 responses in DCMU-poisoned leaves. The slower CO_2 closing response of stomata in DCMU-fed G132 leaves may be due to the impaired functioning of the slow anion channel SLAH3. Although some changes in the population of individual ion channels are ineffective and have counterintuitive effects [51, 64], the speed of stomatal movements can be modified through the manipulation of the ion channels in guard cells. Elevated stomatal conductance, as displayed by G132, is a trait that could increase photosynthesis in well-watered conditions.

Acknowledgements

A.L. Verdejo contributed to plant growth and gas exchange and ATP measurements. We thank Dr. Xavier Aranda from IRTA for his contribution in promoting the selection of different barley mutants in a growth chamber at elevated CO_2, and Dr. Sreenivasulu (Leibniz Institute of Plant Genetics and Crop Plant Research-IPK, Gatersleben, Germany) for his help with the RNA microarrays. This work was funded by the Spanish Research and Development Programme-European Regional Development Fund, ERDF (Projects RTA2009-00006-C04-01 and AGL2009-11987) and the regional government, the Junta de Castilla y León (Projects CSI148A11-2 and CSI250U13). J. Córdoba was the recipient of a pre-doctoral contract from the National Institute of Agricultural and Food Research-INIA.

References

[1] A. Del Pozo, P. Pérez, R. Morcuende, A. Alonso, R. Martínez-Carrasco, Acclimatory responses of stomatal conductance and photosynthesis to elevated CO2 and temperature in wheat crops grown at varying levels of N supply in a Mediterranean environment, Plant Science, 169 (2005) 908-916.
[2] P.J. Franks, M.A. Adams, J.S. Amthor, M.M. Barbour, J.A. Berry, D.S. Ellsworth, G.D. Farquhar, O. Ghannoum, J. Lloyd, N. McDowell, R.J. Norby, D.T. Tissue, S. von Caemmerer, Sensitivity of plants to changing atmospheric CO2 concentration: from the geological past to the next century, The New phytologist, 197 (2013) 1077-1094.
[3] J.W.H. Outlaw, Integration of Cellular and Physiological Functions of Guard Cells, Critical Reviews in Plant Sciences, 22 (2003) 503-529.
[4] J. SÁnchez-RodrÍguez, P. PÉrez, R. MartÍnez-Carrasco, Photosynthesis, carbohydrate levels and chlorophyll fluorescence-estimated intercellular CO2 in water-stressed Casuarina equisetifolia Forst. & Forst, Plant, cell & environment, 22 (1999) 867-873.
[5] T. Vahisalu, H. Kollist, Y.F. Wang, N. Nishimura, W.Y. Chan, G. Valerio, A. Lamminmaki, M. Brosche, H. Moldau, R. Desikan, J.I. Schroeder, J. Kangasjarvi, SLAC1 is required for plant guard cell S-type anion channel function in stomatal signalling, Nature, 452 (2008) 487-491.
[6] E.A. Ainsworth, C.R. Yendrek, S. Sitch, W.J. Collins, L.D. Emberson, The effects of tropospheric ozone on net primary productivity and implications for climate change, Annual review of plant biology, 63 (2012) 637-661.
[7] E. Merilo, I. Joesaar, M. Brosche, H. Kollist, To open or to close: species-specific stomatal responses to simultaneously applied opposing environmental factors, The New phytologist, 202 (2014) 499-508.
[8] G. Farquhar, S. Wong, An Empirical Model of Stomatal Conductance, Functional Plant Biology, 11 (1984) 191-210.
[9] T.D. Sharkey, K. Raschke, Separation and measurement of direct and indirect effects of light on stomata, Plant physiology, 68 (1981) 33-40.
[10] K.A. Mott, Do Stomata Respond to CO(2) Concentrations Other than Intercellular?, Plant physiology, 86 (1988) 200-203.
[11] S.C. Wong, I.R. Cowan, G.D. Farquhar, Stomatal conductance correlates with photosynthetic capacity, Nature, 282 (1979) 424-426.
[12] F.A. Busch, Opinion: the red-light response of stomatal movement is sensed by the redox state of the photosynthetic electron transport chain, Photosynthesis research, 119 (2014) 131-140.
[13] E.A. Ainsworth, A. Rogers, The response of photosynthesis and stomatal conductance to rising [CO2]: mechanisms and environmental interactions, Plant, cell & environment, 30 (2007) 258-270.
[14] S.M. Messinger, T.N. Buckley, K.A. Mott, Evidence for involvement of photosynthetic processes in the stomatal response to CO2, Plant physiology, 140 (2006) 771-778.
[15] M. Tominaga, T. Kinoshita, K. Shimazaki, Guard-cell chloroplasts provide ATP required for H(+) pumping in the plasma membrane and stomatal opening, Plant & cell physiology, 42 (2001) 795-802.
[16] V. Haake, R. Zrenner, U. Sonnewald, M. Stitt, A moderate decrease of plastid aldolase activity inhibits photosynthesis, alters the levels of sugars and starch, and inhibits growth of potato plants, The Plant journal : for cell and molecular biology, 14 (1998) 147-157.

[17] M. Muschak, L. Willmitzer, J. Fisahn, Gas-exchange analysis of chloroplastic fructose-1,6-bisphosphatase antisense potatoes at different air humidities and at elevated CO(2), Planta, 209 (1999) 104-111.
[18] G.D. Price, J.R. Evans, S. von Caemmerer, J.W. Yu, M.R. Badger, Specific reduction of chloroplast glyceraldehyde-3-phosphate dehydrogenase activity by antisense RNA reduces CO2 assimilation via a reduction in ribulose bisphosphate regeneration in transgenic tobacco plants, Planta, 195 (1995) 369-378.
[19] I. Baroli, G.D. Price, M.R. Badger, S. von Caemmerer, The contribution of photosynthesis to the red light response of stomatal conductance, Plant physiology, 146 (2008) 737-747.
[20] G.S. Hudson, J.R. Evans, S. von Caemmerer, Y.B. Arvidsson, T.J. Andrews, Reduction of ribulose-1,5-bisphosphate carboxylase/oxygenase content by antisense RNA reduces photosynthesis in transgenic tobacco plants, Plant physiology, 98 (1992) 294-302.
[21] W.P. Quick, U. Schurr, R. Scheibe, E.D. Schulze, S.R. Rodermel, L. Bogorad, M. Stitt, Decreased ribulose-1,5-bisphosphate carboxylase-oxygenase in transgenic tobacco transformed with "antisense" rbcS : I. Impact on photosynthesis in ambient growth conditions, Planta, 183 (1991) 542-554.
[22] S. von Caemmerer, T. Lawson, K. Oxborough, N.R. Baker, T.J. Andrews, C.A. Raines, Stomatal conductance does not correlate with photosynthetic capacity in transgenic tobacco with reduced amounts of Rubisco, Journal of experimental botany, 55 (2004) 1157-1166.
[23] T. Lawson, S. Lefebvre, N.R. Baker, J.I. Morison, C.A. Raines, Reductions in mesophyll and guard cell photosynthesis impact on the control of stomatal responses to light and CO2, Journal of experimental botany, 59 (2008) 3609-3619.
[24] S. Frechilla, L.D. Talbott, E. Zeiger, The CO2 response of Vicia guard cells acclimates to growth environment, Journal of experimental botany, 53 (2002) 545-550.
[25] R.J. Lodge, P. Dijkstra, B.G. Drake, J.I.L. Morison, Stomatal acclimation to increased CO2 concentration in a Florida scrub oak species Quercus myrtifolia Willd, Plant, cell & environment, 24 (2001) 77-88.
[26] L.D. Talbott, A. Srivastava, E. Zeiger, Stomata from growth-chamber-grown Vicia faba have an enhanced sensitivity to CO2, Plant, cell & environment, 19 (1996) 1188-1194.
[27] G.D. Price, S.v. Caemmerer, J.R. Evans, K. Siebke, J.M. Anderson, M.R. Badger, Photosynthesis is strongly reduced by antisense suppression of chloroplastic cytochrome *bf* complex in transgenic tobacco, Functional Plant Biology, 25 (1998) 445-452.
[28] H. Hu, A. Boisson-Dernier, M. Israelsson-Nordstrom, M. Bohmer, S. Xue, A. Ries, J. Godoski, J.M. Kuhn, J.I. Schroeder, Carbonic anhydrases are upstream regulators of CO2-controlled stomatal movements in guard cells, Nature cell biology, 12 (2010) 87-93; sup pp 81-18.
[29] M.R. Roelfsema, K.R. Konrad, H. Marten, G.K. Psaras, W. Hartung, R. Hedrich, Guard cells in albino leaf patches do not respond to photosynthetically active radiation, but are sensitive to blue light, CO2 and abscisic acid, Plant, cell & environment, 29 (2006) 1595-1605.
[30] M. Hashimoto, J. Negi, J. Young, M. Israelsson, J.I. Schroeder, K. Iba, Arabidopsis HT1 kinase controls stomatal movements in response to CO2, Nature cell biology, 8 (2006) 391-397.

[31] S. Xue, H. Hu, A. Ries, E. Merilo, H. Kollist, J.I. Schroeder, Central functions of bicarbonate in S-type anion channel activation and OST1 protein kinase in CO2 signal transduction in guard cell, The EMBO journal, 30 (2011) 1645-1658.
[32] J. Negi, O. Matsuda, T. Nagasawa, Y. Oba, H. Takahashi, M. Kawai-Yamada, H. Uchimiya, M. Hashimoto, K. Iba, CO2 regulator SLAC1 and its homologues are essential for anion homeostasis in plant cells, Nature, 452 (2008) 483-486.
[33] E. Merilo, K. Laanemets, H. Hu, S. Xue, L. Jakobson, I. Tulva, M. Gonzalez-Guzman, P.L. Rodriguez, J.I. Schroeder, M. Brosche, H. Kollist, PYR/RCAR receptors contribute to ozone-, reduced air humidity-, darkness-, and CO2-induced stomatal regulation, Plant physiology, 162 (2013) 1652-1668.
[34] D. Geiger, T. Maierhofer, K.A. Al-Rasheid, S. Scherzer, P. Mumm, A. Liese, P. Ache, C. Wellmann, I. Marten, E. Grill, T. Romeis, R. Hedrich, Stomatal closure by fast abscisic acid signaling is mediated by the guard cell anion channel SLAH3 and the receptor RCAR1, Science signaling, 4 (2011) ra32.
[35] T.H. Kim, M. Bohmer, H. Hu, N. Nishimura, J.I. Schroeder, Guard cell signal transduction network: advances in understanding abscisic acid, CO2, and Ca2+ signaling, Annual review of plant biology, 61 (2010) 561-591.
[36] J. Cordoba, P. Perez, R. Morcuende, R. Martinez-Carrasco, J.L. Molina-Cano, Physiological features of a barley mutant with improved response to high CO2, in: N. Vieira, N. Saibo, M.M. Oliveira (Eds.) XIII Congresso Luso-Espanhol de Fisiologia Vegetal. Abstract Book, Sociedade Portuguesa de Fisiologia Vegetal, Oeiras (Portugal), 2013, p. 87.
[37] J.C. Zadoks, T.T. Chang, C.F. Konzak, A decimal code for the growth stages of cereals, Weed Research, 14 (1974) 415-421.
[38] P. Perez, G. Rabnecz, Z. Laufer, D. Gutierrez, Z. Tuba, R. Martinez-Carrasco, Restoration of photosystem II photochemistry and carbon assimilation and related changes in chlorophyll and protein contents during the rehydration of desiccated Xerophyta scabrida leaves, Journal of experimental botany, 62 (2011) 895-905.
[39] S.P. Long, C.J. Bernacchi, Gas exchange measurements, what can they tell us about the underlying limitations to photosynthesis? Procedures and sources of error, Journal of experimental botany, 54 (2003) 2393-2401.
[40] G.D. Farquhar, S. von Caemmerer, J.A. Berry, A biochemical model of photosynthetic CO2 assimilation in leaves of C 3 species, Planta, 149 (1980) 78-90.
[41] L. Gu, S.G. Pallardy, K. Tu, B.E. Law, S.D. Wullschleger, Reliable estimation of biochemical parameters from C(3) leaf photosynthesis-intercellular carbon dioxide response curves, Plant, cell & environment, 33 (2010) 1852-1874.
[42] K.A. Mott, Opinion: stomatal responses to light and CO(2) depend on the mesophyll, Plant, cell & environment, 32 (2009) 1479-1486.
[43] O.H. Lowry, J.V. Passonneau, CHAPTER 9 - A COLLECTION OF METABOLITE ASSAYS, in: O.H.L.V. Passonneau (Ed.) A Flexible System of Enzymatic Analysis, Academic Press, 1972, pp. 146-218.
[44] D.A. Benson, K. Clark, I. Karsch-Mizrachi, D.J. Lipman, J. Ostell, E.W. Sayers, GenBank, Nucleic acids research, 43 (2015) D30-35.
[45] T.J. Close, P.R. Bhat, S. Lonardi, Y. Wu, N. Rostoks, L. Ramsay, A. Druka, N. Stein, J.T. Svensson, S. Wanamaker, S. Bozdag, M.L. Roose, M.J. Moscou, S. Chao, R.K. Varshney, P. Szucs, K. Sato, P.M. Hayes, D.E. Matthews, A. Kleinhofs, G.J. Muehlbauer, J. DeYoung, D.F. Marshall, K. Madishetty, R.D. Fenton, P. Condamine, A. Graner, R. Waugh, Development and implementation of high-throughput SNP genotyping in barley, BMC genomics, 10 (2009) 582.

[46] M. Lohse, A. Nagel, T. Herter, P. May, M. Schroda, R. Zrenner, T. Tohge, A.R. Fernie, M. Stitt, B. Usadel, Mercator: a fast and simple web server for genome scale functional annotation of plant sequence data, Plant, cell & environment, 37 (2014) 1250-1258.
[47] R. Morcuende, A. Krapp, V. Hurry, M. Stitt, Sucrose-feeding leads to increased rates of nitrate assimilation, increased rates of α-oxoglutarate synthesis, and increased synthesis of a wide spectrum of amino acids in tobacco leaves, Planta, 206 (1998) 394-409.
[48] T.D. Schmittgen, K.J. Livak, Analyzing real-time PCR data by the comparative C(T) method, Nature protocols, 3 (2008) 1101-1108.
[49] Y. Benjamini, Controlling the False Discovery Rate: A Practical and Powerful Approach to Multiple testing, 1995.
[50] J.I.L. Morison, Stomatal response to increased CO2 concentration, Journal of experimental botany, 49 (1998) 443-452.
[51] T. Lawson, M.R. Blatt, Stomatal size, speed, and responsiveness impact on photosynthesis and water use efficiency, Plant physiology, 164 (2014) 1556-1570.
[52] P.L. Drake, R.H. Froend, P.J. Franks, Smaller, faster stomata: scaling of stomatal size, rate of response, and stomatal conductance, Journal of experimental botany, 64 (2013) 495-505.
[53] M. Stitt, R.M. Lilley, H.W. Heldt, Adenine nucleotide levels in the cytosol, chloroplasts, and mitochondria of wheat leaf protoplasts, Plant physiology, 70 (1982) 971-977.
[54] T.N. Buckley, K.A. Mott, G.D. Farquhar, A hydromechanical and biochemical model of stomatal conductance, Plant, cell & environment, 26 (2003) 1767-1785.
[55] A.J. Jarvis, W.J. Davies, The coupled response of stomatal conductance to photosynthesis and transpiration, Journal of experimental botany, 49 (1998) 399-406.
[56] K.A. Mott, D.G. Berg, S.M. Hunt, D. Peak, Is the signal from the mesophyll to the guard cells a vapour-phase ion?, Plant, cell & environment, 37 (2014) 1184-1191.
[57] T. Fujita, K. Noguchi, I. Terashima, Apoplastic mesophyll signals induce rapid stomatal responses to CO2 in Commelina communis, The New phytologist, 199 (2013) 395-406.
[58] K.A. Mott, E.D. Sibbernsen, J.C. Shope, The role of the mesophyll in stomatal responses to light and CO2, Plant, cell & environment, 31 (2008) 1299-1306.
[59] S.C. Wong, I.R. Cowan, G.D. Farquhar, Leaf Conductance in Relation to Rate of CO(2) Assimilation: I. Influence of Nitrogen Nutrition, Phosphorus Nutrition, Photon Flux Density, and Ambient Partial Pressure of CO(2) during Ontogeny, Plant physiology, 78 (1985) 821-825.
[60] K. Laanemets, B. Brandt, J. Li, E. Merilo, Y.F. Wang, M.M. Keshwani, S.S. Taylor, H. Kollist, J.I. Schroeder, Calcium-dependent and -independent stomatal signaling network and compensatory feedback control of stomatal opening via Ca2+ sensitivity priming, Plant physiology, 163 (2013) 504-513.
[61] H. Kollist, M. Nuhkat, M.R. Roelfsema, Closing gaps: linking elements that control stomatal movement, The New phytologist, 203 (2014) 44-62.
[62] K. Laanemets, Y.F. Wang, O. Lindgren, J. Wu, N. Nishimura, S. Lee, D. Caddell, E. Merilo, M. Brosche, K. Kilk, U. Soomets, J. Kangasjarvi, J.I. Schroeder, H. Kollist, Mutations in the SLAC1 anion channel slow stomatal opening and severely reduce K+ uptake channel activity via enhanced cytosolic [Ca2+] and increased Ca2+ sensitivity of K+ uptake channels, The New phytologist, 197 (2013) 88-98.
[63] Y. Wang, M. Papanatsiou, C. Eisenach, R. Karnik, M. Williams, A. Hills, V.L. Lew, M.R. Blatt, Systems dynamic modeling of a guard cell Cl- channel mutant

uncovers an emergent homeostatic network regulating stomatal transpiration, Plant physiology, 160 (2012) 1956-1967.
[64] Y. Wang, A. Hills, M.R. Blatt, Systems analysis of guard cell membrane transport for enhanced stomatal dynamics and water use efficiency, Plant physiology, 164 (2014) 1593-1599.

Table 1. Chlorophyll fluorescence quenching parameters and ATP content (µmol g Fwt^{-1}) in barley (*Hordeum vulgare* L.) leaves. The youngest fully expanded leaf of WT (4^{th} leaf) and its G132 mutant (3^{rd} leaf) grown in a glasshouse (chlorophyll fluorescence) and a controlled environment chamber (ATP). Fluorescence was measured with ambient CO_2 concentration (390 µmol mol^{-1}) and 1000 µmol m^{-2} s^{-1} irradiance. Chamber conditions as in Fig. 2. The data are the means (± standard errors) of five replicates. lsd, least significant difference. Numbers in bold type represent significant effects (P<0.05).

	Fv/Fm	Fq'/Fm'	qL	Φ_{NPQ}	ATP
G132	0.52 (0.06)	0.14 (0.01)	0.43 (0.03)	0.73 (0.04)	0.28 (0.05)
WT	0.81 (0.003)	0.36 (0.01)	0.43 (0.03)	0.50 (0.01)	0.17 (0.03)
lsd	**0.101**	**0.045**	0.130	**0.082**	**0.091**

Table 2. Regression parameters and probabilities in the analysis of parallelism of the g_s-time (s) response curves for barley (*Hordeum vulgare* L.) leaves shown in the indicated figures. A sequence of regression models was fitted to the values for WT and the G132 mutant. The first model to be fitted was a single curve with common parameters for both genotypes. Next, the model was extended to include a different constant parameter (A) for each genotype, giving two parallel curves. All the linear parameters in the following model were different for each genotype. Finally, completely separate curves were fitted, in which all the parameters differed between genotypes. The significant regression model with the highest complexity (shown in bold) was selected.

Experiment	Site	Function	Genotype	Regression parameters						Regression analysis of variance			
				A	B	C	k	D	E	common param.	constant separate	all linear param. separate	all param. separate
1800 µmol mol^{-1} CO_2	Growth chamber	$g_s=A+B\cdot\exp^{(k\cdot time)}+C\cdot time$	WT	80.76	51.01	-5.47E-03	-4.13E-03			<.001	<.001	0.831	**0.036**
(Fig. 5c, d)			G132	16.00	150.00	3.13E-02	-7.02E-04						
	Glasshouse		WT	38.33	74.04	-3.00E-03	-3.95E-03			<.001	<.001	<.001	**<.001**
			G132	49.70	139.20	3.58E-03	-1.07E-03						
DCMU (Fig. 6a)	Glasshouse	$g_s=A+(B+C\cdot time)/$ $(1+D\cdot time+E\cdot time^2)$	WT	147.60	49.67	-6.91E-03		-4.15E-04	9.32E-08	<.001	<.001	**<.001**	0.658
			G132	120.60	67.13	-1.58E-02		-4.15E-04	9.32E-08				
50 µmol mol^{-1} CO_2 with DCMU (Fig. 6b)	Glasshouse	$g_s=A+B\cdot\exp^{(k\cdot time)}$	WT	198.00	-49.26		-3.10E-04			<.001	**<.001**		0.315
			G132	162.40	-49.26		-3.10E-04						
800 µmol mol^{-1} CO_2	Glasshouse	$g_s=A+(B+C\cdot time)/$	WT	44.17	54.32	-6.15E-03		-2.82E-04	2.28E-08	<.001	<.001	**<.001**	0.227
with DCMU (Fig. 6b)		$(1+D\cdot time+E\cdot time^2)$	G132	22.08	42.44	-4.48E-03		-2.82E-04	2.28E-08				

Table 3. log2-tranformed transcript level ratios of the barley (*Hordeum vulgare* L.) G132 mutant compared with WT. Primary leaves at the stage of 2 unfolded leaves in plants grown in a controlled environment chamber (conditions as in Fig. 2) were analysed with a microarray, and the youngest fully expanded leaves at the stages of 3 (G132)-4 (WT) leaves from controlled environment-growth plants and of 5 (G132)-7 (WT) leaves from glasshouse-grown plants were analysed by qRT-PCR. Unigene code from HarvEST: Barley v.1.83, Assembly 35 database.

Unigene	Description	GenBank	Log_2 fold change		
			Growth chamber array	Growth chamber qRT-PCR	Glasshouse qRT-PCR
38703	Slow anion channel-associated malate transporter SLAH3 (SLAC1 HOMOLOGUE 3)	AK368060	**-2.23**	**-3.76**	**-0.85**

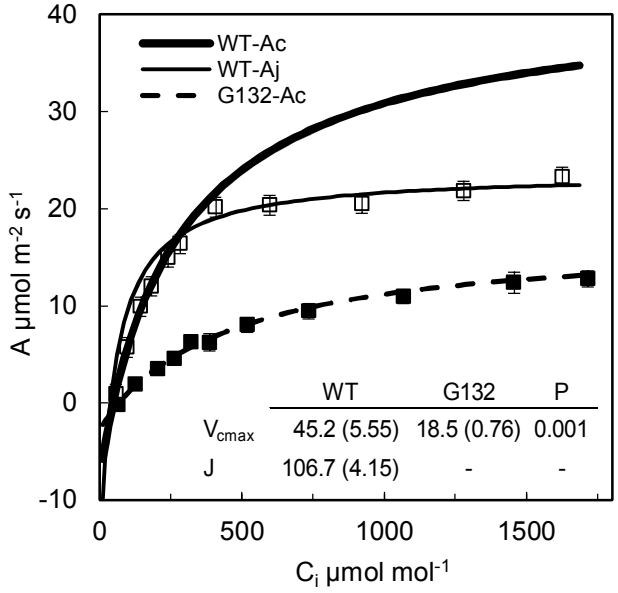

Fig. 1. Rate of CO_2 assimilation limited by Rubisco (A_c) and by Ribulose-1, 5-bisphosphate regeneration (RuBP, A_j) in barley (*Hordeum vulgare* L.). Measured and fitted values for the G132 mutant (closed symbols, broken line) and WT (open symbols, solid lines). There was no RuBP-limited CO_2 assimilation in G132 (see text for details). Curves were fitted with the LeafWeb (leafweb.ornl.gov) utility to five replicate leaves per genotype and the mean values are presented. The youngest fully expanded leaves (3^{rd}-4^{th} leaf) of plants grown in a glasshouse were measured. Vertical bars represent twice the standard error of means. Inset: V_{cmax} and J values (µmol m^{-2} s^{-1} ± standard errors of means) and probability (P) in the analysis of variance.

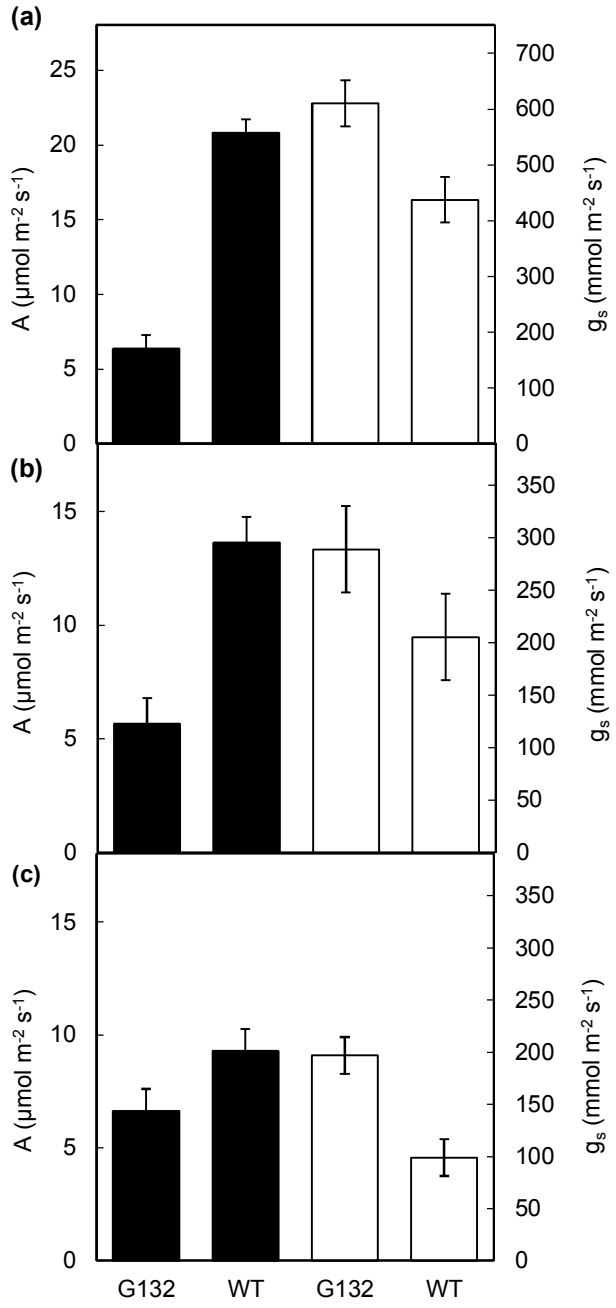

Fig. 2. Photosynthesis (black columns) and stomatal conductance (open columns) of barley (*Hordeum vulgare* L.) leaves. The youngest fully expanded leaf of barley WT and G132 mutant at the stage of (a, b) 3 (G132)-4 (WT) expanded leaves; and (c) 5 (G132)-7 (WT) expanded leaves. Measurements with 390 µmol mol^{-1} CO_2 and 1000 µmol m^{-2} s^{-1} irradiance. Plants were grown in (a) a controlled environment chamber with 390 µmol mol^{-1} CO_2, 20:15 ºC light:dark temperature, 16:8 h light:dark photoperiod, 60 % relative humidity and 450 µmol m^{-2} s^{-1} light intensity; and (b, c) a glasshouse. The data are means of five replicates. Vertical bars represent least significant differences (lsd; $P<0.05$).

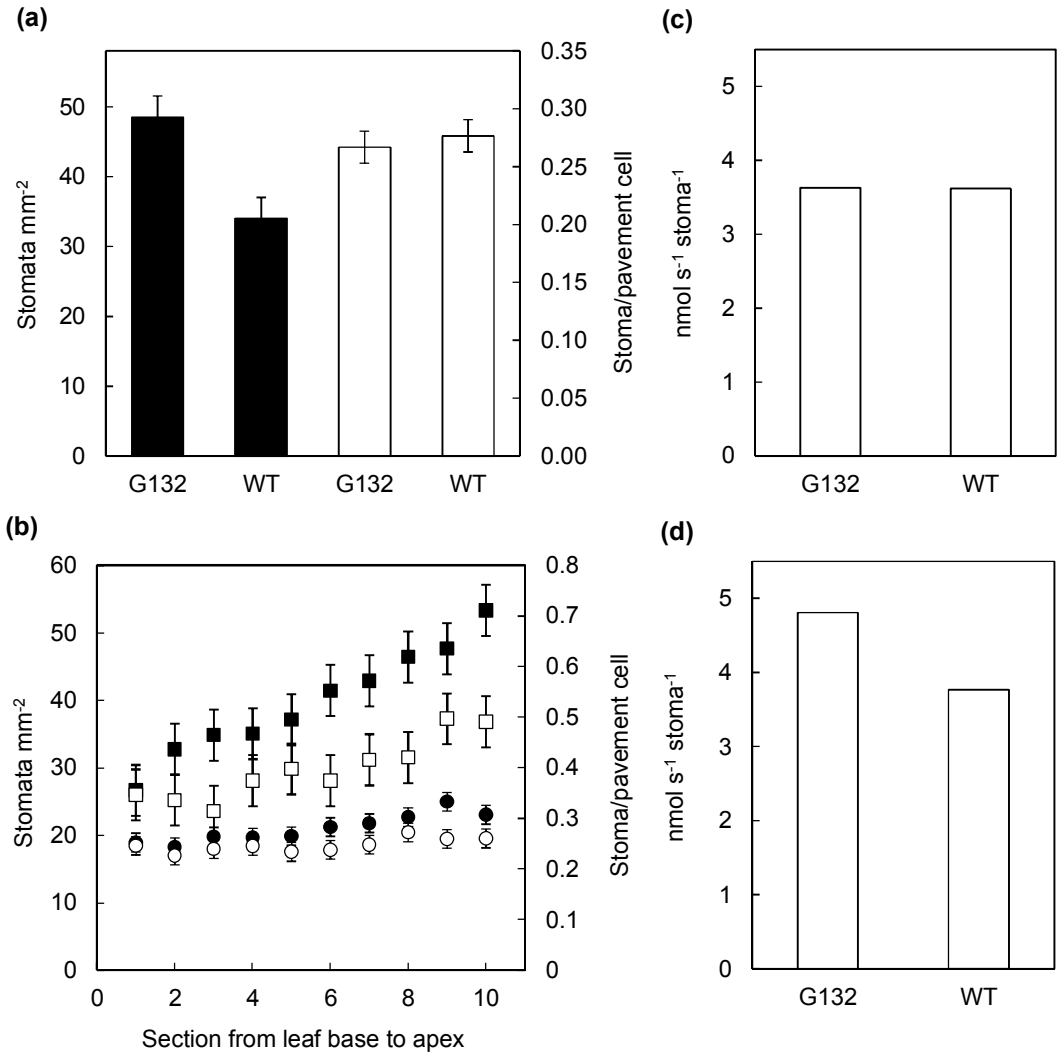

Fig. 3. Stomatal numbers and normalized conductance in barley (*Hordeum vulgare* L.) leaves. (a) Stomatal density (filled columns) and index (open columns) on the adaxial central segment of the youngest fully expanded leaf (3rd [G132]-4th [WT]) of plants grown in a controlled environment chamber with conditions as for Fig. 2; (b) Stomatal density (squares) and index (circles) along the adaxial side of the youngest fully expanded leaf (5th [G132, filled symbols]-7th [WT, open symbols]) of plants grown in a glasshouse. Conductance normalized to stomatal density in the adaxial central segment of (c) growth chamber-plants and (d) glasshouse-plants. The steady state stomatal conductance was determined after 20 min in an atmosphere with 390 µmol mol^{-1} CO_2, 1000 µmol m^{-2} s^{-1} red irradiance, 0.95±0.12 kPa vapour pressure deficit and 20 ºC. Each point is the mean of five replicate leaves. Vertical bars represent the lsd (P<0.05).

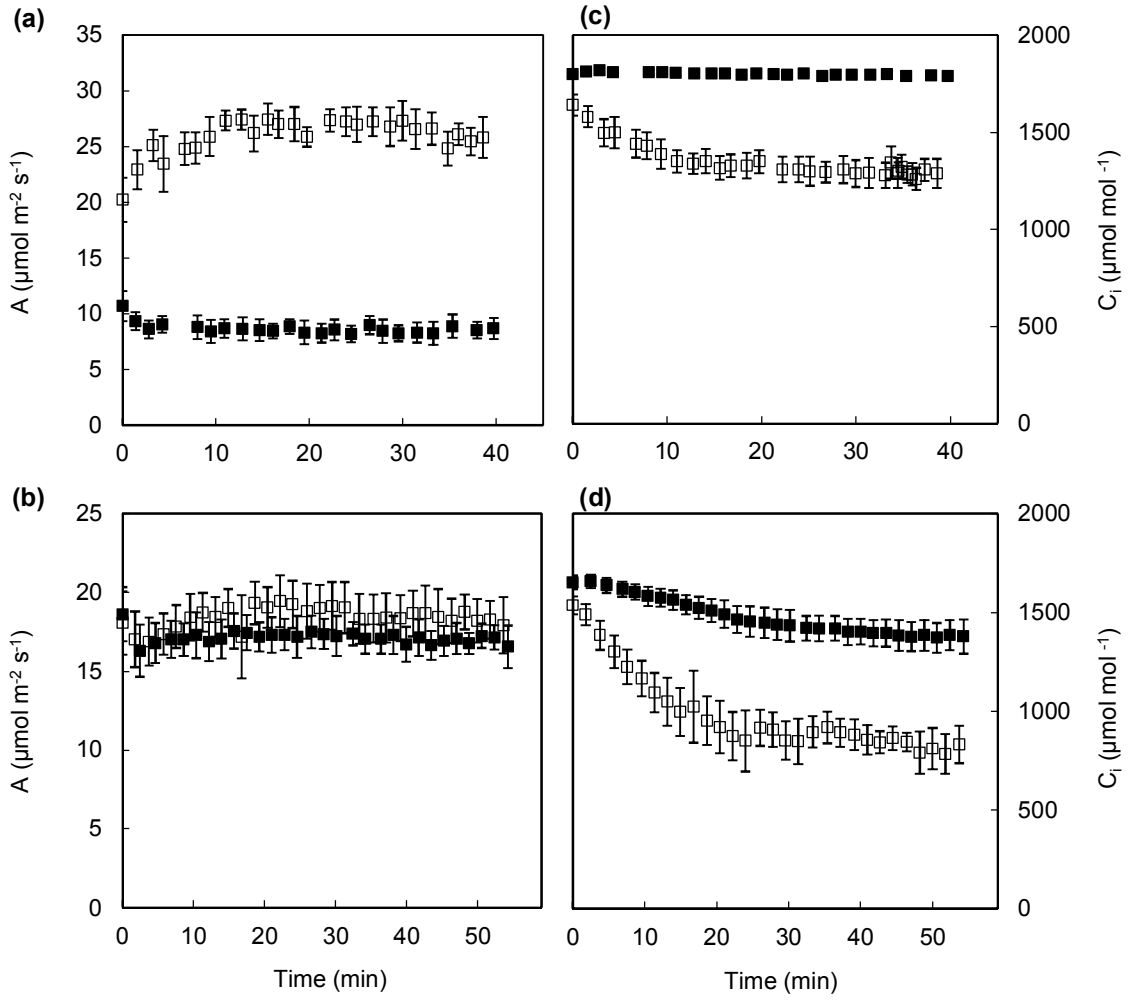

Fig. 4. Change with time in photosynthesis and intercellular CO_2 concentration of barley (*Hordeum vulgare* L.) leaves after a step increase in air CO_2 concentration. CO_2 was increased from 390 to 1800 µmol mol^{-1} under 1000 µmol m^{-2} s^{-1} red irradiance at time zero. (a, b) photosynthesis and (c, d) intercellular CO_2 concentration of the youngest fully expanded leaves of the G132 mutant (closed squares) and WT (open squares) at the growth stage of (a, c) 3 (G132)-4 (WT) leaves in a controlled environment chamber with conditions as for Fig. 2; (b, d) 5 (G132)-7 (WT) leaves in a glasshouse. Mean of five replicate leaves per genotype. Vertical bars represent twice the standard errors of means.

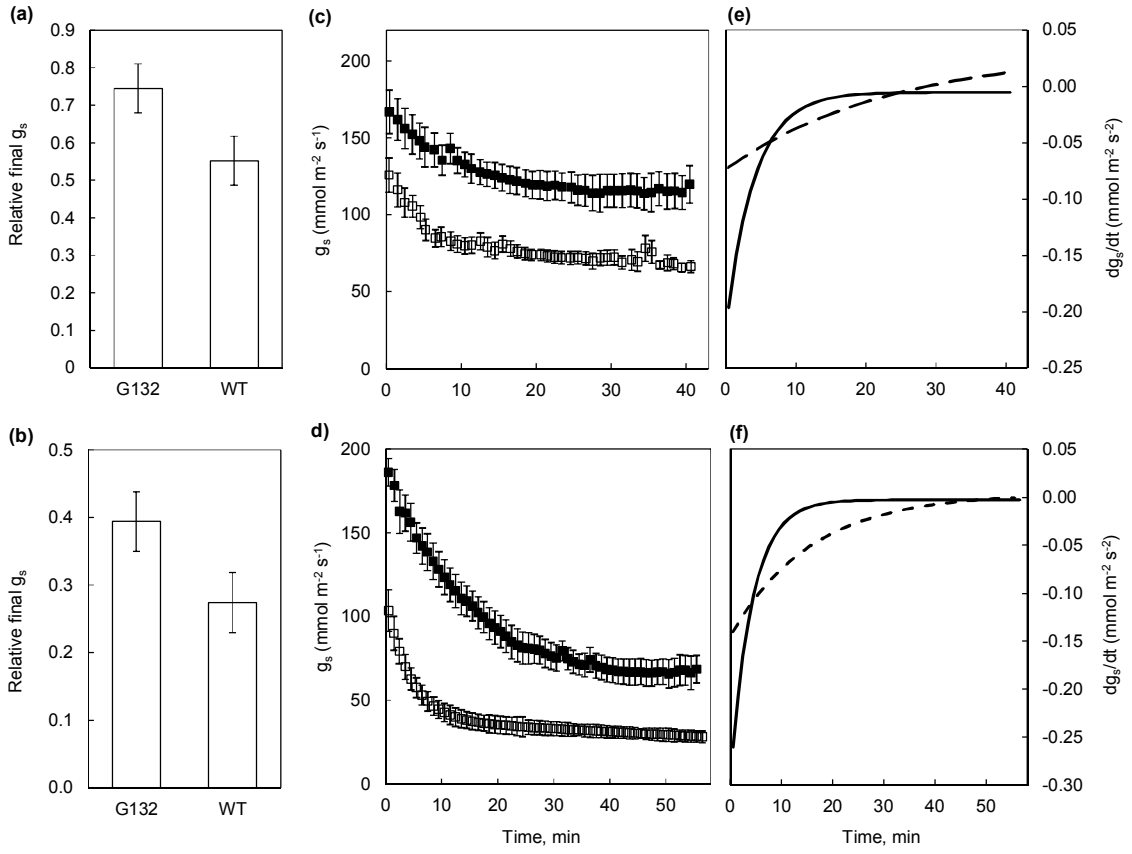

Fig. 5. Stomatal conductance of barley (*Hordeum vulgare* L.) leaves after a step increase of air CO_2 concentration. CO_2 was increased from 390 to 1800 µmol mol^{-1} under 1000 µmol m^{-2} s^{-1} red irradiance at time zero. Measurements in the youngest fully expanded leaves of the G132 mutant (closed squares, dashed lines) and WT (open squares, closed lines) at the growth stage of (a, c, e) 3 (G132)-4 (WT) leaves in a controlled environment chamber with conditions as for Fig. 2, and of (b, d, f) 5 (G132)-7 (Graphic) leaves in a glasshouse. (a, b) g_s after 40-50 min in 1800 µmol mol^{-1} CO_2 relative to initial g_s. (c, d) Change with time in stomatal conductance. Regressions of g_s over time with the shape (exponential plus linear) $g_s=A+B\cdot\exp^{(k\cdot time)}+C\cdot time$ were fitted. Table 2 shows the regression parameters and statistical significance (analysis of parallelism) of the differences between genotypes. (e, f) Rates of g_s change over time, estimated as first derivatives with respect to time of curves in panels (c) and (d), respectively. Means of five replicate leaves per genotype. Vertical bars represent twice the standard errors of means.

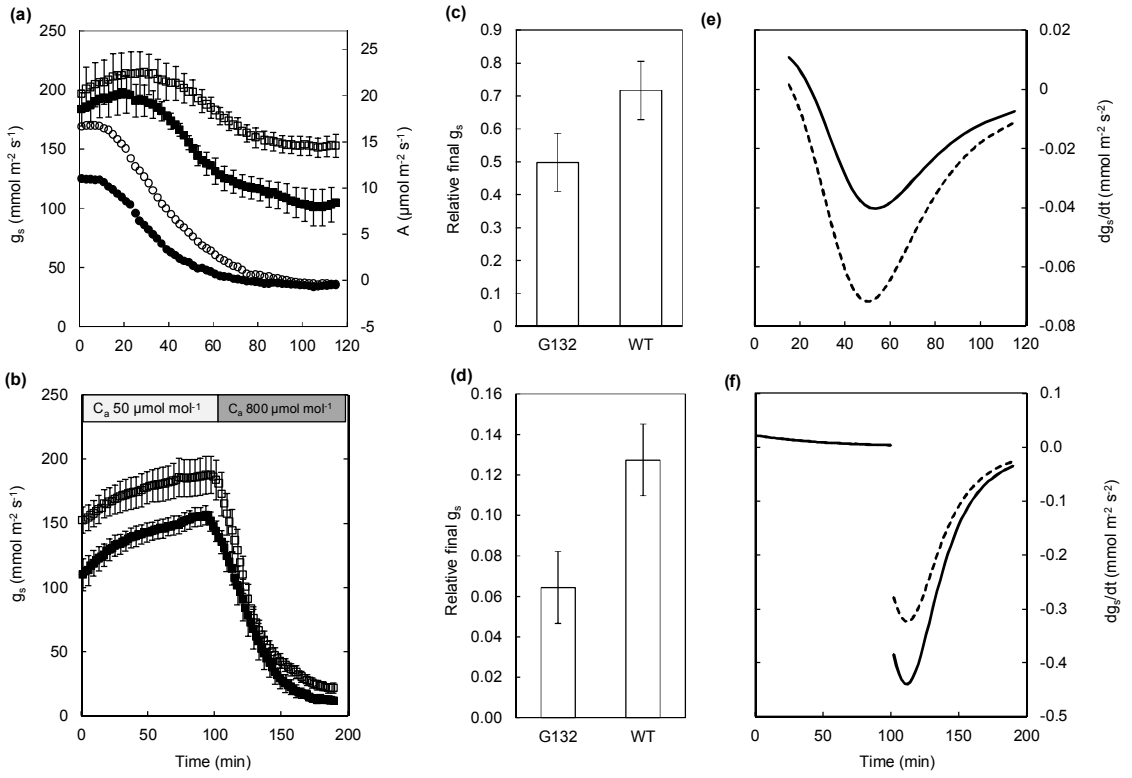

Fig. 6. Photosynthesis (circles) and stomatal conductance (squares) of leaves of the barley (*Hordeum vulgare* L.) mutant G132 (closed symbols, dashed lines) and WT (open symbols, solid lines) in response to DCMU feeding and air CO_2 concentration. (a) DCMU (100 µM) was supplied at zero time to detached leaves kept at 390 µmol mol^{-1} CO_2 under 1000 µmol m^{-2} s^{-1} red light; C_i was held constant by decreasing C_a; (b) C_a was decreased from 390 to 50 µmol mol^{-1} CO_2 and subsequently increased to 800 µmol mol^{-1} CO_2, following the exposure to DCMU shown in panel (a). Regressions were fitted to g_s change over time; Table 2 shows the regression parameters and statistical significance (analysis of parallelism) of the differences between the G132 mutant and WT. (c, d) final g_s relative to initial g_s after (c) DCMU feeding at 390 µmol mol^{-1} CO_2; (d) increasing CO_2 from 50 to 800 µmol mol^{-1}. (e, f) Rates of g_s change over time, estimated as first derivatives with respect to time of curves in panels (a) and (b), respectively. The youngest fully expanded leaf (5th leaf) of glasshouse-grown plants. The data are the means of six replicate leaves per genotype. Vertical bars represent twice the standard errors of means.